10.21608/adjc.2024.343170.1677 Advanced Dental Journal
Volume 7 (2025) | Issue 4| Pages 734-744 ©Faculty of Dentistry-Cairo University

Original Article

Cellulose nanocrystals/zinc oxide nanoparticles for Enhanced Antifungal Activity and Flexural Properties of a Heat-cured Acrylic Denture Base Material

Samar Shokri Ibrahim [1], Farid Abd-Elrheim Badria [2], Nahed Galal Bakir [3]

[1]Biomaterials Department, Faculty of Dentistry, October 6 University, Egypt
[2]Pharmacognosy Department, Faculty of Pharmacy, Mansoura University, Egypt
[3]Biomaterials Department, Faculty of Dentistry, Cairo University, Egypt

Email: samar.ibrahim@dentistry.cu.edu.eg

Submitted: 09-12-2024
Accepted: 26-12-2024

Abstract

Aim: To develop an antifungal heat-cured acrylic denture base material with enhanced flexural strength, by incorporating a nanohybrid of nanocellulose and nano zinc oxide into the acrylic.
Subjects and methods: Zn^{2+} was precipitated on the surface of nanocellulose to create a nanohybrid of nanocellulose and nano zinc oxide. The nano zinc oxide, nanocellulose, and nanohybrid were evaluated for particle size and surface morphology using transmission and scanning electron microscopy respectively, and their structure was determined using X-ray diffraction. Two groups of specimens were prepared: unmodified conventional acrylic resin (control), and 1.1% w/w nanohybrid-modified acrylic (intervention). In each group, nine cylindrical specimens were prepared to evaluate antifungal activity using agar dilution method, and eleven bar-shaped specimens for determination of three-point flexural strength and modulus using a Universal Testing Machine.
Results: In 1/10 and 1/100 dilutions, incorporating the nanohybrid into the conventional heat-cured acrylic significantly reduced *Candida* colonies count and led to a notable improvement in both flexural strength (93.38 ± 7.34 MPa for the modified vs. 44.89 ± 4.06 MPa for the unmodified group) and modulus (2257.78 ± 168.37 MPa for the modified vs. 1373.26 ± 209.69 MPa for the unmodified group).
Conclusion: Incorporating 1.1% w/w of the nanohybrid into conventional heat-cured acrylic resin may be considered a viable approach to provide antifungal activity and enhance flexural strength and modulus.

Keywords: Denture base, Cellulose nanocrystals, Zinc oxide nanoparticles, antifungal activity, flexural strength.

Introduction

Tooth loss affects the patients' speech, mastication, appearance, and social life, increasing the demand for an ideal substitute to restore the patients' functional and esthetic loss. For both therapeutic and financial reasons, a removable acrylic resin denture is still the most common prosthetic solution (Rahaman Ali *et al.*, 2020). Despite the long history of clinical success of poly(methyl methacrylate) acrylic resin, it has drawbacks such as lack of antimicrobial activity, the main cause of denture stomatitis, and inferior mechanical properties making them highly prone to fracture either during service due to their low

flexural strength, or when accidentally dropped due to their low impact strength (Gad *et al.*, 2019).

The incorporation of various nanoparticles into the PMMA has been approached to overcome the drawbacks of PMMA denture base materials. Zinc oxide (ZnO) possesses superior properties as biocompatibility, nontoxic properties, optical transparency, electrical conductivity, and low cost. Nano-sized particles of ZnO have been reported to possess pronounced antimicrobial activities compared to large size particles (Król *et al.*, 2017). In order to enhance the mechanical properties of acrylic resin, different reinforcing materials such as fibers, fillers and nanofillers have been incorporated into PMMA (Gad *et al.*, 2017).

The recent shift towards the usage of natural products in the dental field, is related to their biocompatible properties, renewable resources, biohazards-free nature, and cost-effectiveness compared to synthetic products (Rahaman Ali *et al.*, 2020).

Cellulose, an important structural component of the cell wall of multiple plants, is the most abundant natural polymer available on earth. Cellulose nanocrystals (CNCs), also known as whiskers, needles or nanoparticles are highly crystalline rod-like nanostructures that are obtained by acid hydrolysis of any natural source of cellulose. Its most accepted nomenclature is CNCs (Owoyokun *et al.*, 2021). CNCs possess many desirable properties such as superior mechanical properties, low density, renewable and nonabrasive nature which permit easy processing and an abundance of surface hydroxyl groups, allowing their use as reinforcement elements in different materials (Grishkewich *et al.*, 2017).

Since the incorporation of zinc oxide nanoparticles (ZnO NPs) into acrylic resin rendered antifungal and antibacterial activity (Albuquerque *et al.*, 2023), and the addition of CNCs improved the mechanical properties (Aupaphong *et. al,* 2022), thus a nanohybrid of CNCs and ZnO NPs was thought off to impart antimicrobial activity and enhance the flexural properties. Therefore, the aim of the current study was to develop an antifungal heat-cured acrylic denture base material with enhanced flexural properties, by incorporating a nanohybrid of nanocellulose and nano zinc oxide into the acrylic.

Subjects and Methods

Materials used in the current study were zinc nitrate hexahydrate, sodium hydroxide, Microcrystalline Cellulose (MCC) of plant origin (Loba Chemie, Mumbai, India), and a conventional heat-cured PMMA acrylic resin denture base material (Acrostone, Egypt).

1. Preparation of ZnO NPs, CNCs, and (CNCs/ZnO NPs) nanohybrid:

Zinc nitrate hexahydrate ($Zn(NO_3)_2 \bullet 6H_2O$) and sodium hydroxide (NaOH) were used to precipitate zinc oxide nanoparticles following **Rudeerat Suntako** (Suntako, 2015).

CNCs and (CNCs/ZnO NPs) nanohybrid were prepared at Nanogate, Cairo, Egypt, following the technique described by **Yazi Wang** (Wang *et al.*, 2019). Two grams of Microcrystalline Cellulose (MCC) were soaked into 100 mL mixed acid, prepared by mixing 90 mL of 3 mol/L citric acid and 10 mL of 6 mol/L HCl, to hydrolyse the amorphous regions of MCC allowing the crystalline regions to become the domain structure (Fornari et al., 2022). Fischer esterification was carried out using citric acid to obtain CNC functionalized with -COOH (CNC-COOH) (Yu *et al.*, 2019).

In order to prepare (CNCs/ZnO NPs) nanohybrid, 22.41 mL of the prepared zinc nitrate hexahydrate solution was added to the CNC-COOH suspension, and 8.96 mL NaOH solution (0.5 mol/L) was added dropwise to precipitate Zn^{2+} on the surface of CNCs to obtain the nanohybrid.

2. Characterization of ZnO NPs, CNCs, and (CNCs/ZnO NPs) nanohybrid:

The particle size of ZnO NPs, CNCs, and (CNCs/ZnO NPs) nanohybrid was assessed using Transmission electron microscopy (TEM) (JEOL JEM-2100) at an accelerating voltage of 200 kV. Their structure was identified by X-ray diffraction (XRD) (XPERT-PRO Powder Diffractometer system) with 2θ (10^O - 80^O), a minimum step size 2θ = 0.001, and at a wavelength (Kα) = 1.54614^O.

3. Determination of the minimal inhibitory concentration (MIC) of (CNCs/ZnO NPs) nanohybrid:

MIC of (CNCs/ZnO NPs) nanohybrid against *C. albicans* was determined by double fold serial dilution following **Sadoon and Al-noori, (2022)** to detect the lowest concentration inhibiting the visible growth of *C. albicans.* A stock solution (test tube #1) was prepared by dissolving a 500 mg of (CNCs/ZnO NPs) nanohybrid in 2 mL of Dimethyl sulfoxide. Test tubes were labeled from 1 to 5, and 1 mL of Dimethyl sulfoxide was dispensed in each test tube from no. 2 to no. 5. Double fold serial dilution was performed.

4. Specimen preparation:

Modification of PMMA powder was carried out by gentle hand mixing of 0.25g; 1.1% w/w (CNCs/ZnO NPs) nanohybrid powder, based on MIC results, with 21.75g conventional heat-cured acrylic resin powder using a mortar and pestle. Following manufacturer's instructions, twenty-two grams of polymer powder and 10 mL of liquid monomer, a powder/ liquid ratio of 3/1 by volume, were mixed. Compression molding technique was used for the preparation of heat polymerized specimens of both the unmodified and the (CNCs/ZnO NPs) nanohybrid-modified PMMA specimens (S. El-Din *et al.*, 2018). Two groups of specimens: unmodified (control) and modified (intervention) groups, 20 specimens /group, were prepared.

Scanning electron microscopy and energy-dispersive X-ray (TESCAN VEGA3, Czech Republic) were used to examine the surface morphology and analyze the elemental composition of (CNCs/ZnO NPs) nanohybrid added to PMMA powder as well as that of nanohybrid-modified heat-cured specimen. The distribution of (CNCs/ZnO NPs) in PMMA matrix was explored by elemental mapping.

5. Antifungal evaluation:

A total of 18 cylindrical specimens (4mm in diameter and 4mm in height), nine specimens of each group, were prepared using a split Teflon mold. The specimens were autoclaved and immersed in distilled water at room temperature, 30±2˚C for 8 hours, followed by 16 hours immersion in artificial saliva at 37˚C. This immersion protocol would mimic the common practice of immersing a denture in water for 8 hours at night then wearing it for the rest of the day. This immersion protocol was repeated for one week prior to testing to allow leaching out of the excess residual monomer from the acrylic resin specimens (Quezada *et al.*, 2021).

The agar dilution method was performed as described by **Hany *et al*., 2020**. For obtaining the inoculum, *C. albicans* (Laboratory of Microbiology, Faculty of Medicine, Cairo University) were replicated in Mueller Hinton Broth and incubated at 37 ºC for 24 hours. Both the unmodified and modified heat-cured specimens were inserted in test tubes containing *C. albicans* with 0.5 McFarland standards and incubated at 37 °C for 24 hours with continuous shaking to distribute the *Candida*.

a. Determination of Colony forming units (CFU):

Paper points were used to obtain swabs from the surface of each acrylic resin specimen and were then transferred to test tubes containing 1 ml Mueller Hinton Broth. Two dilutions of the Broth were used (1/10 and 1/100). Twenty microliters of the Broth from each tube were then aspirated and introduced into special plates containing Sabouraud Agar media using micro pipettes. The plates were incubated at 37°C for 48 hours. Finally, CFU were manually counted for both dilutions.

b. Biofilm assay of *C. albicans*:

Scanning electron microscopy (FEI Quanta

FEG 250, USA) was used to examine the biofilm formed on the specimens' surfaces after immersion in *C. albicans* and incubation for 48 hours (Abualsaud *et al.*, 2021).

6. Flexural properties testing:

Specimens for the flexural strength evaluation were prepared according to the ADA specification No. 12 for denture base polymers (American Dental Association, 1975). A total of 22 bar shaped specimens (65 × 10 × 2.5 mm); 11 from each group, were prepared using a Teflon mold. Prior to testing, the specimens were immersed in distilled water at 37± 1˚C for 50±2 hours. Three-point flexure test was carried out using a Universal Testing Machine (Model 3345, Instron, England) following the ISO specification # 1567:1999 for denture base polymers (Gharechahi *et al.*, 2014).

The flexural strength (S) in MPa was calculated as $S = 3WL/2bd^2$ where **W** is the load in Newton, at the point of fracture, **L** is the distance between the two supports in mm, **b** is specimen width in mm, and **d** is specimen thickness in mm.

The flexural modulus (E) in MPa, was automatically calculated as $E = FL^3/4Ybd^3$ where **F** is the maximum load in Newton, and **Y** is the deflection in mm (Sakaguchi R.L. *et al*., 2012).

7. Statistical Analysis:

Data were analyzed using Medcalc software, version 19 for windows (MedCalc Software Ltd, Ostend, Belgium). Data were explored for normality using Kolmogrov Smirnov test and Shapiro Wilk test. Continuous data showed normal distribution and the results were described as means and standard deviations. Pairwise comparisons were done using independent t test with statistical significance set at $P \leq 0.05$. All tests were two tailed.

Results

1. Characterization of ZnO NPs, CNCs, and (CNCs/ZnO NPs) nanohybrid:

The TE micrograph of ZnO NPs showed spheroidal, spherical, and hexagonal particles with an average particle size of 80±10 nm whereas that of CNCs showed nanosheets with an average thickness less than 10 nm forming a porous network. Moreover, in the TE micrograph of (CNCs/ZnO NPs) nanohybrid, the ZnO NPs appears conjugated onto CNC nanosheets **(Figure 1)**.

The XRD patterns of ZnO, CNCs, and CNCs/ZnO **(Figure 2)** exhibited two sets of diffraction peaks for CNCs and ZnO, respectively, as well as separate peaks in the 2θ region that correspond to a hexagonal wurtzite structure of ZnO and Iβ cellulose with a monoclinic crystalline structure.

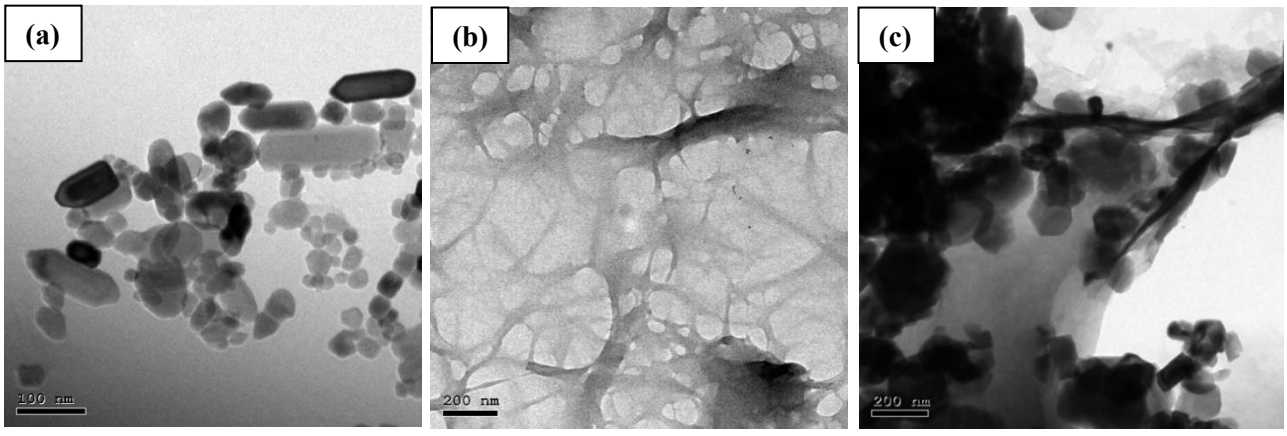

Figure 1: TE micrographs showing (a) spheroidal, spherical and hexagonal ZnO NPs, (b) nanosheets with a porous network of CNCs, and (c) ZnO NPs conjugated onto nanosheets of CNCs

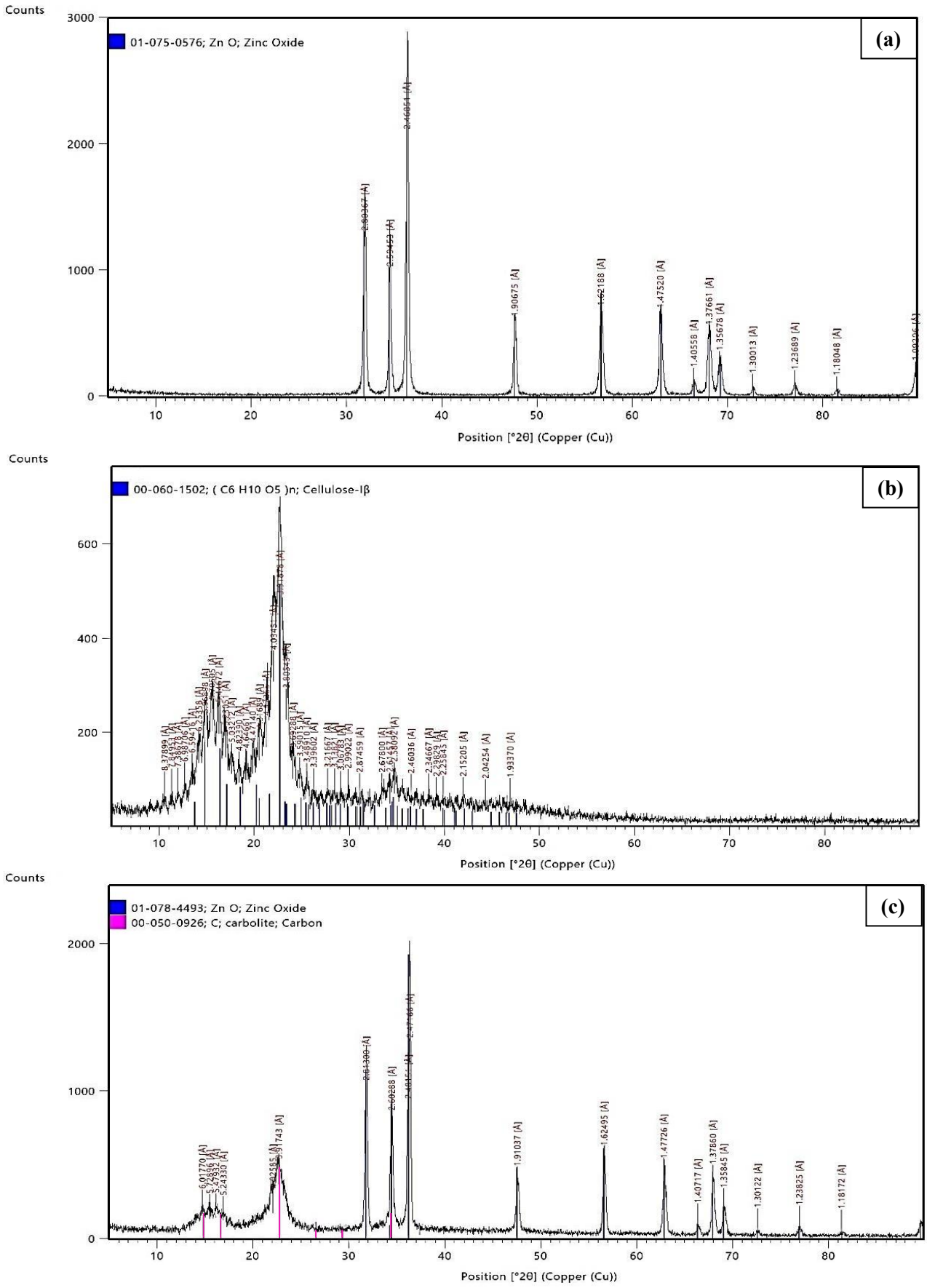

Figure 2: XRD patterns of (a) ZnO NPs, (b) CNCs, and (c) (CNCs/ZnO NPs) nanohybrid

2. Detection of (CNCs/ZnO NPs) nanohybrid in PMMA:

The SE micrograph **(Figure 3)** showed rod-like (CNCs/ZnO NPs) nanohybrid powder distributed in the PMMA powder. Meanwhile, it was not possible to detect the (CNCs/ZnO NPs) nanohybrid in heat-cured PMMA matrix.

EDX analysis of both (CNCs/ZnO NPs) nanohybrid powder mixed with PMMA powder, and the nanohybrid-modified heat-cured acrylic resin **(Figure 3)** revealed the presence of peaks at 0.3, 0.5 and 1.0 keV corresponding to carbon, oxygen and zinc.

The dispersion of (CNCs/ZnO NPs) in the matrix of cured PMMA specimen, as detected by elemental mapping, is shown in **(Figure 4)**. Carbon, oxygen and zinc signals are scattered all over the PMMA matrix.

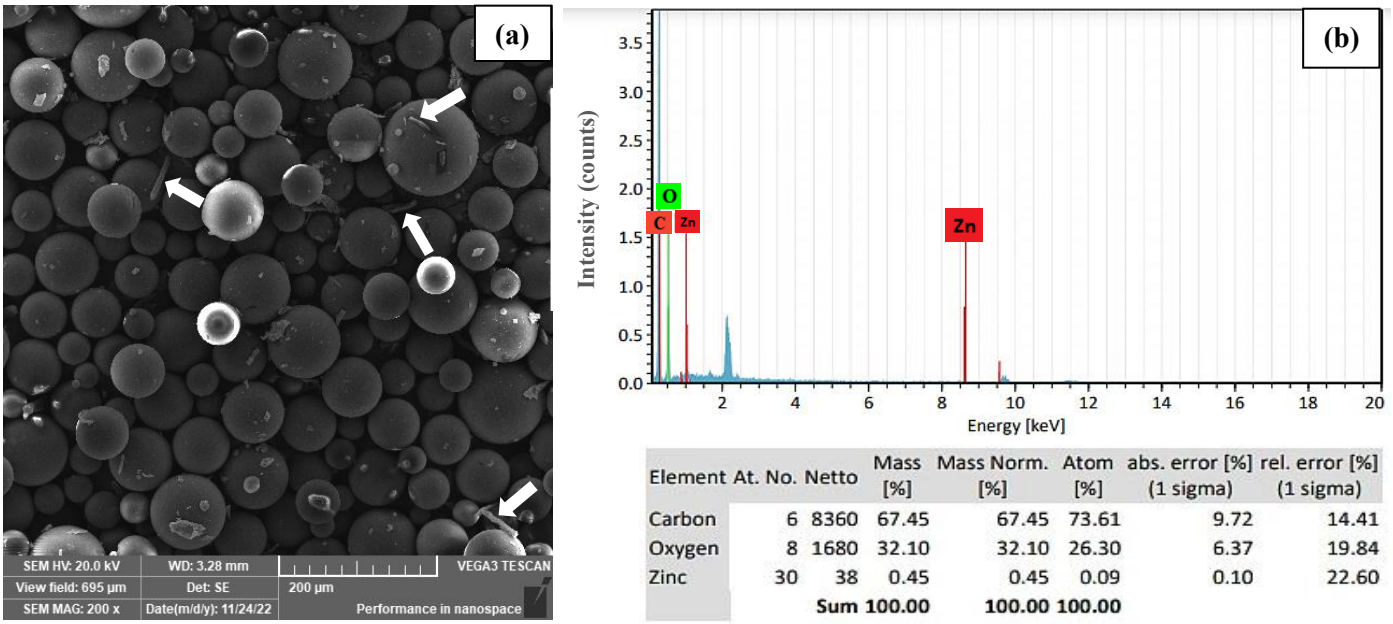

Element	At. No.	Netto	Mass [%]	Mass Norm. [%]	Atom [%]	abs. error [%] (1 sigma)	rel. error [%] (1 sigma)
Carbon	6	8360	67.45	67.45	73.61	9.72	14.41
Oxygen	8	1680	32.10	32.10	26.30	6.37	19.84
Zinc	30	38	0.45	0.45	0.09	0.10	22.60
		Sum	100.00	100.00	100.00		

Figure 3: The (CNCs/ZnO NPs) nanohybrid powder mixed with PMMA powder: (a) SE micrograph at 200 x magnification. Arrows are pointing at the rod-like shape of the (CNCs/ZnO NPs) nanohybrid. (b) EDX analysis

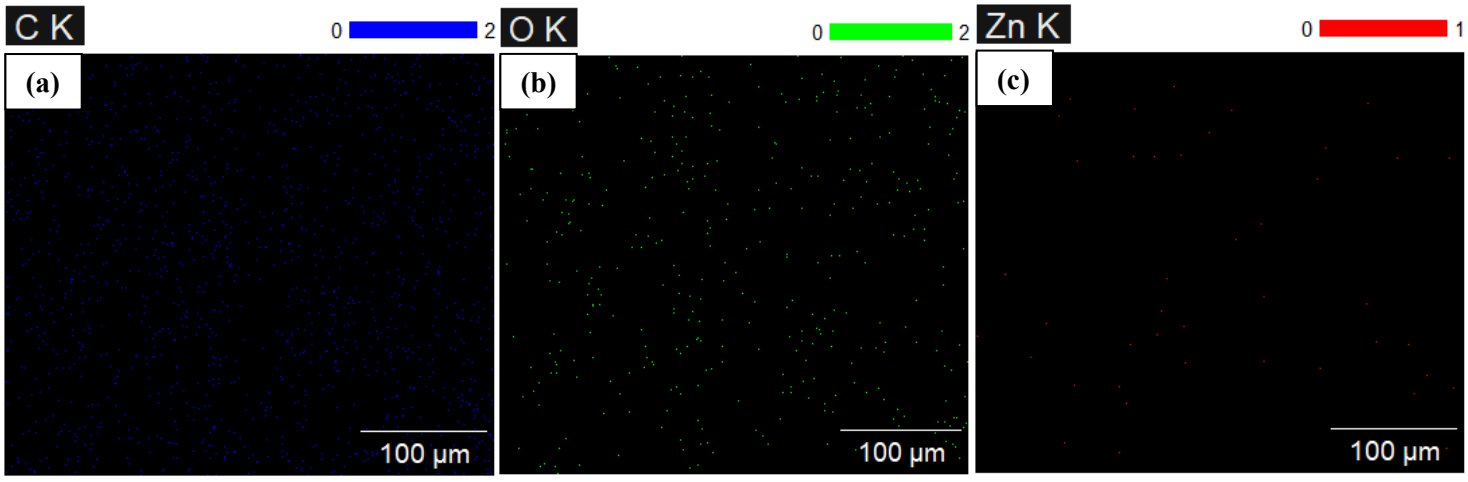

Figure 4: Elemental mapping showing, (a) blue carbon signals, (b) green oxygen signals, and (c) red zinc signals in PMMA matrix

3. MIC of (CNCs/ZnO NPs) nanohybrid against *C. albicans*:

C. albicans (CFU) equal to 8, 5 and 3 corresponded to (CNCs/ZnO NPs) nanohybrid concentrations of 31.25, 62.5 and 125 mg/ml. The highest inhibition, zero *C. albicans* (CFU) corresponded to nanohybrid concentrations of 250 and 500 mg/ml, i.e., the determined MIC is equal to 250 mg/ml (0.25 g).

4. Antifungal evaluation:

a. Candida count (CFU):

A significant reduction in the *Candida* count in (CFU) was evident in both 1/10 dilution (58.55 ± 14.89 for the modified acrylic resin vs. 283.33 ± 78.42 for the unmodified resin, $P < 0.0001$), and 1/100 dilution (16.44 ± 7.53 for modified vs. 149.55 ± 89.10 for the unmodified acrylic resin, $P = 0.0004$), (**Figure 5).**

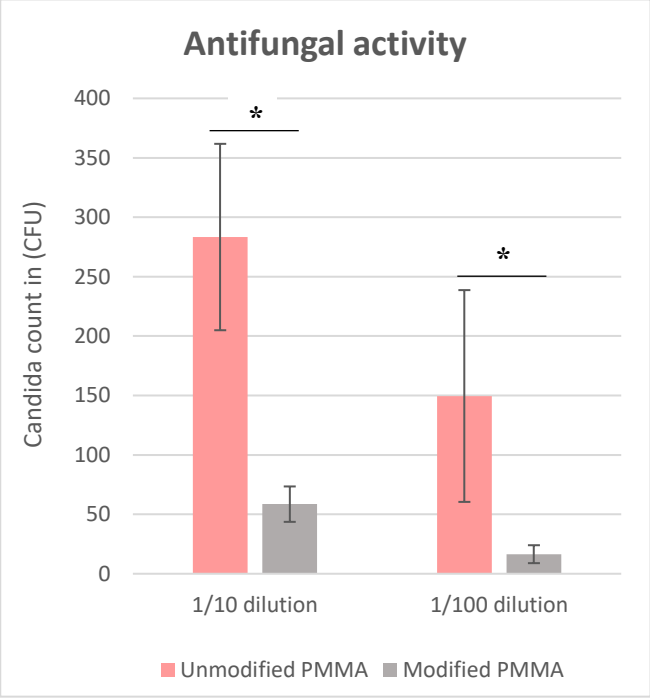

Figure 5: Bar chart representing CFU by agar dilution method with dilutions of 1/10 and 1/100 for the control and the intervention groups. The asterisk (*) indicates significant difference between two groups

b. Biofilm observation by SEM:

In the SE micrographs (**Figure 6),** a large extent of fungal cells with extended filamentous hyphae was observed on the surface of the unmodified acrylic resin. On the contrary, the biofilm architecture was damaged on the surface of (CNCs/ZnO NPs)-modified acrylic resin, with few deformed *C. albicans* cells and damaged hyphae.

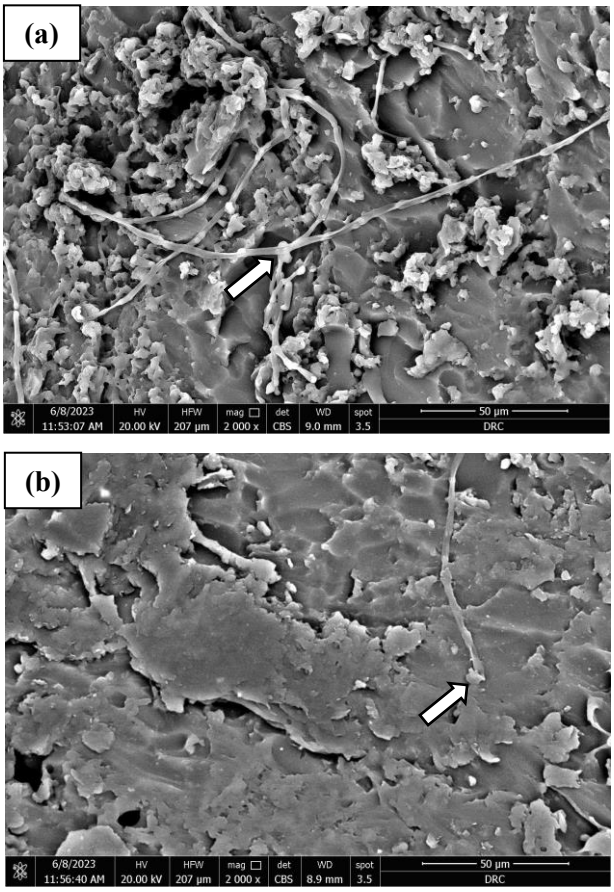

Figure 6: SE micrographs showing *C. albicans* cells on (a) the unmodified acrylic resin specimens' surface, and (b) the nanohybrid-modified specimens' surface at 2000x magnification. The arrows are pointing at *C. albicans* cells

5. Flexural properties:

Results showed a significant improvement in both flexural strength and modulus in the modified acrylic resin group compared to the control group, (**Table 1).**

Table (1): Means and standard deviations of flexural strength and modulus; in MPa, of the control and the intervention groups

Group	Unmodified PMMA		Modified PMMA		P value
	Mean	SD	Mean	SD	
Flexural strength	44.89	4.06	93.38	7.34	P < 0.0001*
Flexural modulus	1373.26	209.69	2257.78	168.37	P < 0.0001*

**Significant difference at P≤0.05.*

Discussion

Modified CNCs can be created by functionalizing cellulose nanocrystals, which are crystalline nanostructures with a large number of surface hydroxyl groups. The metallic nanoparticles will adhere to the surface of CNCs because of the electrostatic contact between them and the oxygen atoms of the hydroxyl groups. In order to create the nanohybrid, CNCs can therefore absorb Zn^{2+} (Farooq *et al.*, 2020).

Because of the abundance of hydroxyl groups on the surfaces of CNCs; which will make it challenging for them to disperse uniformly into the hydrophobic polymer matrices, cellulose nanocrystals are hydrophilic. By producing CNCs with reduced hydrophilicity, Fischer esterification modification will improve the interfacial adhesion and compatibility with the hydrophobic matrix, which may consequently result in improved CNC dispersion into the hydrophobic PMMA matrix (Zhang *et al.*, 2023).

The interactions between the ester functional group ($COOCH_3$) of PMMA and the hydroxyl groups on the surface of CNCs may be considered the mechanism by which (CNCs/ZnO NPs) nanohybrid bind to the PMMA matrix by creating hydrogen bonds (Wasim *et al.*, 2021).

1. Characterization of CNCs, ZnO NPs, and (CNCs/ZnO NPs) nanohybrid:

The TEM results confirmed that the particle size of both CNCs and ZnO NPs are meeting the required conditions for nanomaterials i.e. smaller than 100 nm. The formation of self-assembled CNCs porous networks is due to the strong hydrogen bonding among CNCs which overcomes the repulsive force of their surface negative charges (Lu *et al*., 2010).

The presence of strong and narrow diffraction peaks in the XRD pattern of ZnO NPs indicates the formation of highly crystalline ZnO NPs. The appearance of two sets of diffraction peaks corresponding to the CNCs structure (Zhu *et al.*, 2020) and ZnO in the XRD pattern results (**Figure 2)** further confirms that the (CNCs/ZnO NPs) nanohybrid were successfully prepared (Albuquerque *et al.*, 2023). It could be hypothesized that (CNCs/ZnO NPs) nanohybrid are perfectly compatible and dispersed in the PMMA matrix, so it was difficult to verify the presence of the nanohybrid in the SE micrograph of the modified heat-cured specimen (Leite *et al.*, 2022).

The presence of peaks corresponding to C, O and Zn in EDX analysis; (**Figure 3)** indicates the presence of CNCs and ZnO in the PMMA matrix. The large areas of well dispersed (CNCs/ZnO NPs) nanohybrid in the matrix of cured PMMA in elemental mapping (**Figure 4)** may indicate that (CNCs/ZnO NPs) did not aggregate in the PMMA specimens (Chen *et al.*, 2018).

2. Antifungal activity:

The superior antifungal activity of the modified PMMA may be attributed to the direct contact of ZnO NPs with the cell membrane of the *C. albicans.* This may inhibit the growth of fungi by interfering with the cellular functions and destroying the fungal hyphae (Djearamane *et al.*, 2022).

The antifungal findings of the current study were in agreement with those of **Kamonkhantikul *et al.*, 2017** who concluded that the addition of ZnO NPs into the PMMA would

result in a significant reduction in *C. albicans*. This could be attributed to the uniform distribution of ZnO NPs in PMMA, resulting in a high surface-to-volume ratio thus increasing the contact area between the ZnO NPs and *C. albicans.*

The SE micrograph of the surface of modified acrylic resin specimen, revealed that the (CNCs/ZnO NPs)-modified acrylic resin possess an inhibitory effect on *C. albicans* biofilm formation (**Figure 6**), and this may confirm the antifungal results obtained from the agar dilution method.

3. Flexural properties:

Flexural strength is an important mechanical property as it determines the endurance of the prosthesis. Poor flexural strength increases the incidence of fracture of the denture during service. Moreover, the flexural modulus reflects the material's stiffness and rigidity as well as the ability of the material to equally distribute the forces to the underlying structures (Al-Dwairi *et al.*, 2020).

According to ISO specification # 20795–1:2013, the flexural strength and flexural modulus of a denture base material should be greater than 65 MPa and 2.0 GPa respectively (Kawaguchi *et al.*, 2020). In the current study, the results exceeded the ISO requirements of both the flexural strength and flexural modulus.

The improvement in the flexural strength of the modified PMMA in the current study was similar to that revealed by the addition of 1 wt. % of CNCs to denture reline resin (Silvério *et al.*, 2022). The improvement in mechanical properties could be related to the strong interfacial bonding between the resin matrix and the nanofillers as a consequence to the formation of hydrogen bonds between the hydroxyl groups on CNCs surfaces and the resin matrix as well as the chemical modifications of CNCs to improve the compatibility with the PMMA matrix (Zhang *et al.*, 2023).

Adhesion between the PMMA resin matrix and the CNCs nanofillers may cause efficient stress transfer, resulting in an increase in the strength of acrylic resin. The homogeneity of CNCs within the PMMA matrix prevents the formation of stress concentration points and crack propagation resulting in an improvement in the mechanical properties (Jurado *et al.*, 2023). Moreover, CNCs can restrict the movement of polymer chains, which may enhance the rigidity of PMMA acrylic resin material (Chen *et al.*, 2019).

Conclusion:

Within the study limitations, the following conclusion could be drawn:

Incorporating 1.1% w/w of the (CNCs/ZnO NPs) nanohybrid into conventional heat-cured acrylic resin may be considered a viable approach to provide antifungal activity and enhance flexural strength and modulus.

Conflict of Interest:
The authors declare no conflict of interest.

Funding:
This research received no specific grant from any funding agency in the public, commercial, or not-for-profit sectors.

Ethics:
This study protocol was approved by the ethical committee of the faculty of dentistry-Cairo university on: 29/3/2022, approval number: 8322

Data Availability:
Data will be available upon request.

Clinical trial registration:
This study is an in-vitro study which is not applied on clinicaltrials.gov

Credit statement:
Samar Ibrahim: Data curation, Writing - review & editing, Writing - original draft, Methodology, Resources.
Farid Badria: Conceptualization, Supervision, Writing - review & editing.
Nahed Bakir: Writing - review & editing, Investigation, Formal analysis, Supervision.

References

Abualsaud, R. *et al.* (2021) 'Antifungal Activity of Denture Base Resin Containing Nanozirconia: In Vitro Assessment of Candida albicans Biofilm', *Scientific World Journal*, 2021. doi: 10.1155/2021/5556413.

Al-Dwairi, Z. N. *et al.* (2020) 'A Comparison of the Flexural and Impact Strengths and Flexural Modulus of CAD/CAM and Conventional Heat-Cured Polymethyl Methacrylate (PMMA)', *Journal of Prosthodontics*, 29(4), pp. 341–349. doi: 10.1111/jopr.12926.

Albuquerque, L. A. P. M. *et al.* (2023) 'Efficacy of Chemically and Biologically Synthesized Zinc Oxide Nanoparticles Incorporated in Soft Denture Liner against Candida albicans: A Comparative In Vitro Study', *World Journal of Dentistry*, 14(10), pp. 851–859. doi: 10.5005/jp-journals-10015-2311.

Aupaphong, V., Kraiwattanawong, K. and Thanathornwong, B. (2022) 'Effects of Nanocrystal Cellulose from Bamboo on the Flexural Strength of Acrylic Resin: In Vitro', *Dentistry Journal*, 10(7), pp. 1–10. doi: 10.3390/dj10070129.

Chen, S. *et al.* (2018) 'A study of 3D-printable reinforced composite resin: PMMA modified with silver nanoparticles loaded cellulose nanocrystal', *Materials*, 11(12). doi: 10.3390/ma11122444.

Chen, Y. *et al.* (2019) 'Reinforcing mechanism of cellulose nanocrystals in nanocomposites', *Nanocellulose: From Fundamentals to Advanced Materials*, pp. 201–250. doi: 10.1002/9783527807437.ch7.

Co, E. *et al.* (1975) 'Revised American Dental Association specification no. 12 for denture base polymers.', *Journal of the American Dental Association (1939)*, 90(2), pp. 451–458. doi: 10.14219/jada.archive.1975.0069.

Djearamane, S. *et al.* (2022) 'Antifungal Properties of Zinc Oxide Nanoparticles on Candida albicans', *Coatings*, 12(12), pp. 1–15. doi: 10.3390/coatings12121864.

Farooq, Amjad *et al.* (2020) 'Cellulose from sources to nanocellulose and an overview of synthesis and properties of nanocellulose/zinc oxide nanocomposite materials', *International Journal of Biological Macromolecules*, 154, pp.1050–1073.doi: 10.1016/j.ijbiomac.2020.03.163.

Fornari, A. *et al.* (2022) 'A Review of Applications of Nanocellulose to Preserve and Protect Cultural Heritage Wood, Paintings, and Historical Papers', *Applied Sciences (Switzerland)*, 12(24). doi: 10.3390/app122412846.

Gad, M. M. *et al.* (2017) 'PMMA denture base material enhancement: A review of fiber, filler, and nanofiller addition', *International Journal of Nanomedicine*, 12, pp. 3801–3812. doi: 10.2147/IJN.S130722.

Gad, M. M. *et al.* (2019) 'Reinforcement of PMMA denture base material with a mixture of ZrO 2 nanoparticles and glass fibers', *International Journal of Dentistry*, 2019. doi: 10.1155/2019/2489393.

Gharechahi, J. *et al.* (2014) 'Flexural strength of acrylic resin denture bases processed by two different methods.', *Journal of dental research, dental clinics, dental prospects*, 8(3), pp. 148–52. doi: 10.5681/joddd.2014.027.

Grishkewich, N. *et al.* (2017) 'Recent advances in the application of cellulose nanocrystals', *Current Opinion in Colloid and Interface Science*, 29, pp. 32–45. doi: 10.1016/j.cocis.2017.01.005.

Hany, R. A., Habib, S. I. and Abdelrahman, G. A. (2020) 'Evaluation of the Antifungal Activity on Candida in Siwak Solution Versus Distilled Water', *Egyptian Dental journal*, 1, pp. 457–468.

Jurado-Contreras, S. *et al.* (2023) 'Obtaining Cellulose Nanocrystals from Olive Tree Pruning Waste and Evaluation of Their Influence as a Reinforcement on Biocomposites', *Polymers*, 15(21). doi: 10.3390/polym15214251.

Kamonkhantikul, K., Arksornnukit, M. and Takahashi, H. (2017) 'Antifungal, optical, and mechanical properties of polymethylmethacrylate material incorporated with silanized zinc oxide nanoparticles', *International Journal of Nanomedicine*, 12, pp. 2353–2360. doi: 10.2147/IJN.S132116.

Kawaguchi, T. *et al.* (2020) 'Effect of

cellulose nanofiber content on flexural properties of a model, thermoplastic, injection-molded, polymethyl methacrylate denture base material', *Journal of the Mechanical Behavior of Biomedical Materials*, 102(June 2019), p. 103513. doi: 10.1016/j.jmbbm.2019.103513.

Król, A. *et al.* (2017) 'Zinc oxide nanoparticles: Synthesis, antiseptic activity and toxicity mechanism', *Advances in Colloid and Interface Science*, 249, pp. 37–52. doi: 10.1016/j.cis.2017.07.033.

Leite, A. *et al.* (2022) 'Cellulose nanocrystals into Poly(ethyl methacrylate) used for dental application', *Polímeros*, 32(1), pp. 1–7. doi: 10.1590/0104-1428.20210066.

Lu, P. and Hsieh, Y. Lo (2010) 'Preparation and properties of cellulose nanocrystals: Rods, spheres, and network', *Carbohydrate Polymers*, 82(2), pp. 329–336. doi: 10.1016/j.carbpol.2010.04.073.

Nam, K. Y., Lee, C. H. and Lee, C. J. (2012) 'Antifungal and physical characteristics of modified denture base acrylic incorporated with silver nanoparticles', *Gerodontology*, 29(2), pp. 413–419. doi: 10.1111/j.1741-2358.2011.00489.x.

Owoyokun, T. *et al.* (2021) 'Cellulose nanocrystals: Obtaining and sources of a promising bionanomaterial for advanced applications', *Biointerface Research in Applied Chemistry*, 11(4), pp. 11797–11816. doi: 10.33263/BRIAC114.1179711816.

Quezada-Morales, P. *et al.* (2021) 'Antibacterial Activity of Zinc Oxide Nanoparticles in Self- Curing Acrylic Resin Against Streptococcus mutans', *International journal of odontostomatology*, 15(3), pp. 694–701. doi: 10.4067/s0718-381x2021000300694.

Rahaman Ali, A. A. A. *et al.* (2020) 'Effect of Thermal Cycling on Flexural Properties of Microcrystalline Cellulose-Reinforced Denture Base Acrylic Resins', *Journal of Prosthodontics*, 29(7), pp. 611–616. doi: 10.1111/jopr.13018.

S. El-Din, M. *et al.* (2018) 'Effect of Two Polishing Techniques on Surface Roughness of Three Different Denture Base Materials (an in Vitro Study)', *Alexandria Dental Journal*, 43(3), pp. 34–40. doi: 10.21608/adjalexu.2018.57990.

Sadoon, M. M. and Al-noori, A. K. (2022) 'Effect of Different Nanoparticles Incorporation in Acrylic Based Soft Liner on Candida albicans Adhesion', *Al-Rafidain Dental Journal*, 22(1), pp. 158–169.

Sakaguchi Ronald L. and Powers John M. (2012) *Craig's Restorative Dental Materials*, *Craig's restorative dental materials*. doi: 10.1038/sj.bdj.2012.659.

Silvério, H. A. *et al.* (2022) 'Poly (ethyl methacrylate) composites reinforced with modified and unmodified cellulose nanocrystals and its application as a denture resin', *Polymer Bulletin*, 79(4), pp. 2539–2557. doi: 10.1007/s00289-021-03621-0.

Suntako, R. (2015) 'Effect of zinc oxide nanoparticles synthesized by a precipitation method', *Bulletin of Materials Science*, 38(4), pp. 1033–1038.

Wang, Y. *et al.* (2019) 'Strong antibacterial dental resin composites containing cellulose nanocrystal/zinc oxide nanohybrids', *Journal of Dentistry*, 80(November), pp. 23–29. doi: 10.1016/j.jdent.2018.11.002.

Wasim, M. *et al.* (2021) 'An overview of Zn/ZnO modified cellulosic nanocomposites and their potential applications', *Journal of Polymer Research*, 28(9), pp. 1–19. doi: 10.1007/s10965-021-02689-6.

Yu, H. *et al.* (2019) 'Simple Process to Produce High-Yield Cellulose Nanocrystals Using Recyclable Citric/Hydrochloric Acids', *ACS Sustainable Chemistry and Engineering*, 7(5), pp. 4912–4923. doi: 10.1021/acssuschemeng.8b05526.

Zhang, Yuzhe *et al.* (2023) 'Preparation methods of cellulose nanocrystal and its application in treatment of environmental pollution: A mini-review', *Colloids and Interface Science Communications*, 53(February), p. 100707. doi: 10.1016/j.colcom.2023.100707.

Zhu, W. *et al.* (2020) 'Formaldehyde-free resin impregnated paper reinforced with cellulose nanocrystal (CNC): Formulation and property analysis', *Journal of Applied Polymer Science*, 137(31), pp. 1–10. doi: 10.1002/app.48931.